Three-dimensional adaptive microscopy using embedded liquid lens

Supraja Murali,[1,*] Kevin P. Thompson,[2] and Jannick P. Rolland[1]

[1]*CREOL, The College of Optics and Photonics, University of Central Florida, Orlando, Florida 32816, USA*
[2]*Optical Research Associates, 280 East Foothill Boulevard, Suite 300, Pasadena, California 91107, USA*
**Corresponding author: smurali@creol.ucf.edu*

Received October 27, 2008; accepted November 10, 2008;
posted December 5, 2008 (Doc. ID 102729); published January 13, 2009

We report on the compact optical design of a high-resolution 3D scanning microscope with adaptive optics capability for refocusing with no moving parts designed for clinical research. The optical aberrations arising from refocusing are compensated for as part of the multiconfiguration optical design process. The lateral scanning is provided by a scanning mirror, and the depth scan is provided by an adaptive liquid lens embedded within the microscope as an integrated component of a custom optical design. The microscope achieves a performance of 250 lp/mm—a tenfold increase in performance over a liquid lens used as a standalone optical element. Results show that the optical design provides invariant modular transfer function over a 2 mm × 2 mm × 2 mm imaging volume, fully compensating (i.e., diffraction limited) for dynamic aberrations contributed by the scanning, the variation in the shape of the liquid lens, and the change in spherical aberration with depth in a slab of average index of refraction of skin. This design can find applications in biomedical imaging, white light interferometry for surface roughness measurements, and other 3D imaging systems.

OCIS codes: 220.1080, 220.3620, 170.3880, 170.3890, 170.4500.

The most commonly used mechanism for focusing in optical microscopes is through the mechanical motion of the entire objective. Such motion severely restricts either the speed at which an object can be scanned in depth or the range of depth scanning. A variable focus microscope with no moving parts can provide an efficient, compact, and cost-effective solution for a variety of applications including optical coherence microscopes and white light interferometry systems for surface measurement. Dynamic focusing can be classified as one form of an adaptive optics system, where the adaptive optics element such as a deformable mirror (DM) or a liquid crystal (LC) lens is used as a refocusing mechanism rather than for wavefront sensing aberration correction as it is predominantly employed in the research literature [1]. One such system can be realized by incorporation of an adaptive lens within the optical design of the microscope objective whereby the focus change can be generated through either curvature change or refractive index change within the adaptive lens. In one version of an adaptive lens, a refractive index gradient can be achieved using LC technology [2–4]. The LC lens can achieve large focal length variation and operate at low voltage, as successfully reported [5]. However, larger LC lenses, on the order of a few millimeters, are relatively slow (i.e., response times on the order of seconds). Also the LC lens implementation inherently exhibits significantly large wavelength dispersion and optical anisotropy. Recently, adaptive liquid lenses have been shown to provide higher performance, do not require polarized light, and are becoming readily available at pricing that allows the development of research grade instruments [6]. Liquid lenses can be driven through two different operating mechanisms that result in a change in the curvature of the lens. One method is through electrowetting, where the meniscus formed by two immiscible liquids is controlled through the application of voltage [7–9]. The other method is through mechanical control of the curvature of the lens [6,10–12]. To date the best reported resolution is achieved using adaptive lenses of an aperture size of less than 5 mm [13].

The application of a DM in aberration correction for optical coherence tomography has been investigated by Hermann *et al.* [14] and Zawadzki *et al.* [15], and a transverse resolution of 5–10 and 4 μm, respectively, have been reported. An implementation using a steering mirror and a DM combined with an objective and imaging optics have been reported to enlarge the field of view while preserving the lateral resolution of the system; however, the adaptive optic element is not designed for 3D imaging [16]. To our knowledge, the liquid-lens-based microscope reported in this Letter is the first adaptive liquid-lens-based 3D scanning microscopy imaging system designed for both refocus and built-in aberration compensation across a 2 mm imaging depth. We report here a 2 μm level resolution in all three dimensions of a 2 mm × 2 mm × 2 mm imaging cube for optical coherence microscopy (OCM) application operating at 5 frames/s (currently limited by the CCD readout rate of 12,000 frames/s). The optical design and theoretical and fabricated performance measures indicate that the OCM scanning microscope with a liquid lens integrated into the custom microscope design demonstrates ten times the lateral resolution of the liquid lens when used alone through the focal range.

The microscope optical design was developed in the context of biological tissue imaging with the specific application to OCM with a goal of maintaining constant high lateral and axial resolution throughout a

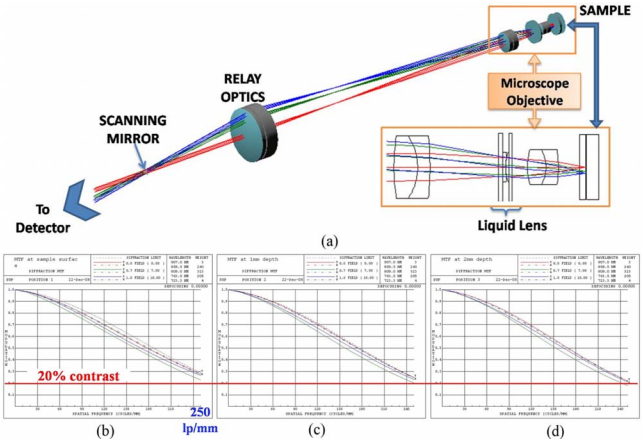

Fig. 1. (Color online) (a) Optical system design layout, (b)–(d) MTF function maps at three focus positions—tissue surface, 1 and 2 mm depths, respectively—show sufficient (>20%) contrast at a spatial frequency of 250 lp/mm.

2 mm×2 mm×2 mm imaging cube. The optical design developed for this prototype was based on an electrowetting technology liquid lens (Varioptic, Arctic 320); the optical design approach is equally applicable to a lens with a mechanical change in curvature. The optical layout of the dynamic focusing microscope objective is shown in Fig. 1. It consists of a Lister-type microscope objective that we adapted to work in immersion in a medium of refractive index of 1.46 such as a glycerol solution that approaches that of the average refractive index of skin. The custom microscope objective was designed to accommodate both the variation in surface curvature of the liquid lens, whose focal length was varied from −2.5 to 16.5 cm and the variation in spherical aberration with focus due to focusing into the skin through a multiconfiguration optimization using optical design software (i.e., CODE V). In addition to the variation in focus, the objective was simultaneously designed to interface with a dual-axis scan mirror and custom relay optics that together enable a 2 mm×2 mm lateral scan. The relay optics was designed to be telecentric using a single doublet. The scan mirror was placed in the exit pupil of the relay optics, thus providing the *en face* scan angle. The system is currently designed to work in a near-infrared broadband spectrum of a bandwidth of 120 nm centered at 800 nm acquired from a Ti:Sa femtosecond pulsed laser source (www.femtolasers.com, INTEGRAL). While the spectrum is considered large for a refractive design, a unique property of the microscope objective design is the use of only two doublets and a glass plate that will come in contact with the skin. The glass materials utilized in this design were chosen to be in the low-to-medium price range, and in regular production, and the design was reduced to a minimum number of elements in order to enable a low-cost, robust, and readily available clinical research tool. Another unique property of the microscope objective optical design is that it was developed to accommodate an integrated liquid lens, where the fixed optics was optimized to compensate for optical aberrations and dispersion within the system including the wavefront errors from the liquid lens as it refocuses, according to its theoretical model provided by the manufacturer, and the variation in spherical aberration caused by the converging beam passing through 0 to 2 mm of skin. Conceptually, it was found possible to balance the spherical aberration induced by the change in bending of the liquid lens as it scans through focus with the change in spherical aberration due to the changing path length in the skin. The dynamic focusing imaging probe is designed to image in 3D at a lateral resolution of 2 μm throughout an 8 mm^3 imaging volume. The axial resolution when used in a broadband low-coherence interferometric setup, such as OCM, is determined by the coherence length of the source, in this case 2.4 μm in air or 1.8 μm in skin. Figure 1(a) provides a cross section of the microscope objective components themselves and a contextual layout for the entire optical system starting at the scan mirror.

Based on the system parameters, the nominal design modular transfer function (MTF) is shown throughout the depth of focus and over the scan in Figs. 1(b)–1(d). Results show that a greater than 20% contrast can be achieved at a spatial frequency of 250 lp/mm consistently throughout the imaging depth [see Figs. 1(b)–1(d)]. A two-point separation of 2 μm (not shown) can be readily resolved throughout the depth of the sample.

A tolerance analysis was conducted in the final stages of the design, and the system was found to be robust to shop-standard fabrication tolerances with less than an 8% drop in MTF contrast overall. Following the final optomechanical design and fabrication, the assembly was tested for output wavefront error using a plane transmission sphere (TS) and a helium neon light source at 632.8 nm in a Zygo interferometric setup as shown in Fig. 2(a). The rms wavefront error achieved by the assembled lens of 0.015 waves rms exceeded the standard definition for diffraction limited of <0.07 waves rms with the liquid lens removed from the system shown in Fig. 2(b), and this diffraction-limited performance was retained with the liquid lens installed as shown in the measurements in Fig. 2(c). The MTF (not shown) is maintained through the focus range for the as fabricated probe. These nominal performance measures demonstrate the success of the fabrication process on meeting alignment specifications as well as fabrication tolerances of the system. Furthermore, the diffraction-limited performance also reflects on the validity of the theoretical model of the liquid lens. The measured data also counteract some industry misconceptions that the wavefront from liquid lenses is not adequate for high-performance imaging applications. While this is often true for liquid lenses used alone, when properly packaged in an integrated optical design the performance of the liquid lens is found to not be a factor that degrades the performance of the system.

We report on a research-grade fabricated prototype of a dynamically refocusing microscope with no moving parts that can achieve invariant 2 μm lateral resolution across an 8 mm^3 cubic volume. While this im-

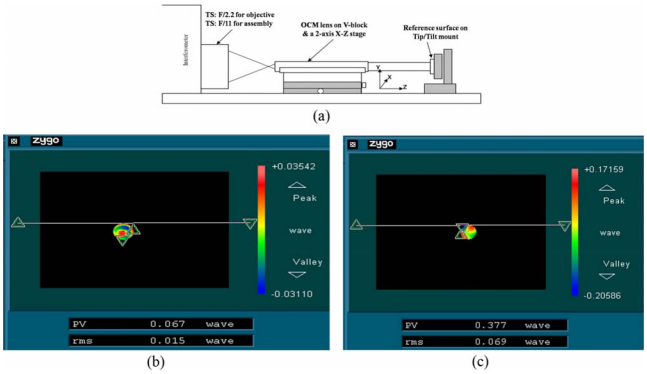

Fig. 2. (Color online) (a) Test setup; output wavefront map of optical system with liquid lens element (b) absent and (c) present, showing diffraction-limited performance.

aging probe was originally devised for its application in clinical research for invariant resolution 3D skin imaging using OCM [17] owing to its high resolution and speed (<100 ms per slice/refocus) it can be extended to a wide range of applications. Importantly, while a typical stand-alone liquid lens is limited to a resolution of 25 lp/mm, when integrated into custom-design optics, an approximately ten times higher resolution is achieved, reaching 250 lp/mm. In the immediate future, we plan to further investigate the effects of the system orientation on the liquid lens curvature caused by gravity and test the probe in a Gabor domain OCM configuration [18].

We acknowledge the Medical Army Research grant for supporting this research, Optical Research Associates for providing the CODEV student license, and General Optics Asia, Ltd. for supporting the optomechanical design and fabrication of the probe.

References

1. M. J. Booth, Philos. Trans. R. Soc. London Ser. A **365**, 2829 (2007).
2. S. Sato, Jpn. J. Appl. Phys. **18**, 1679 (1979).
3. M. Ye and S. Sato, Jpn. J. Appl. Phys., Part 1 **41**, 6407 (2002).
4. S. Murali, K. S. Lee, and J. P. Rolland, Opt. Express **15**, 15854 (2007).
5. H. Ren and S. T. Wu, Opt. Express **14**, 11292 (2006).
6. H. Ren, D. Fox, P. A. Anderson, B. Wu, and S. T. Wu, Opt. Express **14**, 8031 (2006).
7. B. Berge and J. Peseux, Eur. Phys. J. E **3**, 159 (2000).
8. T. Krupenkin, S. Yang, and P. Mach, Appl. Phys. Lett. **82**, 316 (2003).
9. S. Kuiper and B. H. W. Hendriks, Appl. Phys. Lett. **85**, 1128 (2004).
10. G. C. Knollman, J. L. S. Bellin, and J. L. Weaver, J. Acoust. Soc. Am. **49**, 253 (1971).
11. D. Y. Zhang, Appl. Phys. Lett. **82**, 3171 (2003).
12. P. M. Moran, S. Dharmatilleke, A. H. Khaw, K. W. Tan, M. L. Chan, and I. Rodriguez, Appl. Phys. Lett. **88**, 041120 (2006).
13. S. T. Wu, CREOL, The College of Optics and Photonics, University of Central Florida, Orlando, Florida (personal communication, 2007).
14. B. Hermann, E. J. Fernández, A. Unterhuber, H. Sattmann, A. F. Fercher, W. Drexler, P. M. Prieto, and P. Artal, Opt. Lett. **29**, 2142 (2004).
15. R. Zawadzki, S. Jones, S. Olivier, M. Zhao, B. Bower, J. Izatt, S. Choi, S. Laut, and J. Werner, Opt. Express **13**, 8532 (2005).
16. B. Potsaid, Y. Bellouard, and J. Wen, Opt. Express **13**, 6504 (2005).
17. J. A. Izatt, M. R. Hee, G. M. Owen, E. A. Swanson, and J. G. Fujimoto, Opt. Lett. **19**, 590 (1994).
18. J. P. Rolland, P. Meemon, S. Murali, A. Jain, N. Papp, K. Thompson, and K. S. Lee, Proc. SPIE **7139**, 7139OF-1 (2008).